NATIONAL ENGITECH DIGEST

VOL. 3 ISSUE 1

e-ISSN: 3030-5969

Experimental Investigation of the Torsional Behaviour of FDM-Printed PLA under Different Infill Configurations

Nur Raihana Sukri[1*], Siti Zubaidah Abdullah[1], Sutharsanan Ramamurthy[1]

[1]Department of Mechanical Engineering, Politeknik Ungku Omar, Perak, Malaysia

nur_raihana@puo.edu.my, sitizubaidah0826@gmail.com, sutharsananramamurthy@gmail.com

Abstract

This study investigated the torsional behaviour of fused deposition modelling (FDM) polylactic acid (PLA) across four infill densities (15%, 30%, 45% and 60%) and three infill patterns (Honeycomb, Gyroid and Concentric). Thirty-six specimens were tested using a TM201 torsion testing machine, with three replicates for each of the 12 configurations. Maximum recorded torque was analysed for all specimens, while torque at 1800° was compared where complete endpoint measurements were available. Pooled mean maximum torque was 0.734, 0.816, 0.879 and 0.750 N·m at 15%, 30%, 45% and 60%, respectively. Two-factor analysis of variance indicated effects of density, pattern and their interaction (all $p < 0.001$), demonstrating that the response to increasing density depended on pattern. Honeycomb at 45% produced the highest mean maximum torque, 0.970 ± 0.010 N·m, but its mean decreased to 0.527 ± 0.040 N·m at 60%. Gyroid and Concentric means increased to 0.823 ± 0.038 and 0.900 ± 0.026 N·m at 60%, respectively. Concentric at 60% retained 0.840 ± 0.010 N·m at 1800°, approximately 93% of its mean peak torque. These preliminary findings distinguish peak torque from endpoint torque retention and show that higher infill density does not uniformly improve torsional performance. Three replicates per configuration support initial comparisons but do not establish fabrication-wide reproducibility.

Keywords: Fused deposition modelling; polylactic acid; torsional behaviour; infill architecture; additive manufacturing

Introduction

Fused deposition modelling (FDM) is an additive manufacturing technique widely used for producing polymer components because of its low manufacturing cost, accessibility, rapid fabrication capability, and ability to produce complex geometries (Acierno & Patti, 2023). Its application has progressively expanded from rapid prototyping to functional components, customized products, tooling, biomedical applications, and engineering devices (Cano-Vicent et al., 2021). However, the mechanical performance of FDM-printed components differs from that of conventionally manufactured polymers because the final structure consists of deposited material paths and interlayer interfaces separated by internal voids (Rajan et al., 2022).

The mechanical behaviour of FDM components is affected by numerous printing parameters, including material type, layer thickness, printing orientation, raster angle, infill density, and infill pattern (Solomon et al., 2021). In particular, infill density determines the amount of material within the internal structure, while the infill pattern controls the arrangement and load-transfer paths of the deposited material (Tanveer et al., 2022). Consequently, these parameters can significantly affect strength, stiffness, deformation, and failure behaviour (Solomon et al., 2021; Tanveer et al., 2022).

Polylactic acid (PLA) is among the most widely used FDM materials because of its ease of printing, dimensional stability, relatively high stiffness, and availability (Joseph et al., 2023). Previous research has extensively investigated the tensile, compressive, and flexural properties of PLA under different printing conditions (Al-Tamimi et al., 2023). However, comparatively less attention has been given to its torsional response (Sadaghian, 2024). This is important because many functional components, including handles, shafts, couplings, knobs, tools, and assistive devices, experience rotational loading during operation.

Torsional loading generates shear stresses throughout a component and requires effective transfer of load through its internal structure (Kaya & Yaman, 2026). Therefore, an infill configuration that performs well under tensile or flexural loading may not necessarily provide optimum torsional performance. Furthermore, FDM components can experience substantial angular deformation before complete physical failure, making maximum torque alone insufficient to describe their torsional behaviour (Hatwalne & Bhalerao, 2025).

The interaction between infill density and pattern is therefore particularly relevant for designing FDM components subjected to rotational loading (Lumsden et al., 2026). A higher density may increase the available load-bearing material, but excessive material usage may provide diminishing mechanical benefits. Identifying an efficient

combination of density and internal architecture is consequently important for balancing mechanical performance and material consumption.

This study aims to experimentally investigate the torsional behaviour of FDM-printed PLA fabricated using different infill densities and patterns. Specifically, the study evaluates the effects of 15%, 30%, 45% and 60% infill densities and Honeycomb, Gyroid, and Concentric patterns on maximum recorded torque and torque–angle behaviour. The study also examines post-peak behaviour at large angular deformation to provide a more comprehensive assessment of torsional performance.

Methodology

a. Experimental Design and Specimen Fabrication

A 4 × 3 factorial design was used, comprising four infill densities (15%, 30%, 45% and 60%) and three infill patterns (Honeycomb, Gyroid and Concentric). Each configuration contained three separately tested specimens, identified as A, B and C, giving 36 PLA specimens across 12 configurations. All 36 specimen maxima were retained in the peak-torque analysis.

The specimens as shown in Figure 1 were fabricated from PLA using FDM, with printing conditions maintained consistently across the 12 configurations while infill density and pattern were varied. The specimen geometry comprised a cylindrical reduced section of nominal length 60 mm and diameter 6 mm, with enlarged ends for gripping. All configurations used the same specimen geometry to support direct comparison of their recorded torque responses. The analysis focused on component-level torque rather than geometry-normalised shear properties.



Figure 1: Specimens printed using PLA filament.

b. Replication and experimental scale

Three specimens per configuration were used for preliminary screening of the 12 combinations. Replication allows a within-configuration standard deviation to be estimated and avoids representing each configuration by a single test. The balanced design also provides 24 within-configuration residual degrees of freedom for the factorial analysis. These features support an initial comparison under the recorded test conditions.

c. Torsional Testing

Torsional testing was performed using a TM201 torsion testing machine with a maximum capacity of 30 N·m. Each specimen was positioned between the fixtures, aligned with the rotation axis and securely clamped before rotational loading was applied. Torque and angular displacement were recorded in 100° increments, with an endpoint of 1800° where available. Angular displacement refers to recorded machine rotation. Honeycomb 60% specimens A and B have records ending at 1400°, while specimen C has readings through 1800°. Both shorter records were included when calculating maximum torque, but their missing endpoint readings were not extrapolated or imputed.

Maximum recorded torque, T_{max}, was defined as the largest torque reading for each specimen. Torque at 1800°, T_{1800}, describes the late-stage response at a common angular displacement. Maximum torque was used rather than failure torque because a peak or subsequent reduction does not necessarily correspond to complete physical separation. The recorded negative torque readings in Honeycomb 60% were retained as signed instrument readings and were not interpreted as positive residual load capacity or as an independently established failure mechanism.

For configurations with three endpoint readings, torque retention was calculated as $R = 100 \times \text{mean}(T_{1800}) / \text{mean}(T_{max})$. This ratio expresses the mean endpoint torque as a percentage of the configuration mean peak torque. A three-specimen mean endpoint torque and retention ratio were not calculated for Honeycomb 60%, because its A and B records do not contain a reading at 1800°. The sole available endpoint reading, for specimen

C, was −0.36 N·m and is reported separately. Maximum torque and endpoint torque were used as complementary response measures; angle at maximum torque was not included in the comparative statistical analysis.

d. Statistical Analysis

Maximum torque was summarised as mean ± sample standard deviation (SD), with n = 3 for each configuration. A two-factor fixed-effects analysis of variance (ANOVA) evaluated density, pattern and their interaction using all 36 maxima at α = 0.05. The model comprised three density degrees of freedom, two pattern degrees of freedom, six interaction degrees of freedom and 24 residual degrees of freedom. Because the interaction was significant, configuration-specific trends were prioritised over pooled rankings. Separate one-way ANOVAs and Tukey honestly significant difference comparisons were used as supplementary marginal analyses. Pooled density groups contained nine specimens each, while pooled pattern groups contained 12 specimens each. Endpoint results were assessed descriptively and were not included in the peak-torque ANOVA.

Results and Discussion

a. Maximum Recorded Torque

Table 1 reports maximum torque for all 12 configurations. Honeycomb increased from 0.717 ± 0.050 N·m at 15% to 0.970 ± 0.010 N·m at 45%, but decreased to 0.527 ± 0.040 N·m at 60%. This corresponds to a 45.7% reduction from 45% to 60%. In contrast, Gyroid increased from 0.703 ± 0.083 N·m at 15% to 0.823 ± 0.038 N·m at 60%, while Concentric increased from 0.783 ± 0.006 to 0.900 ± 0.026 N·m. Relative to 15%, the increases at 60% were approximately 17.1% for Gyroid and 14.9% for Concentric. Thus, the complete density range shows a non-monotonic response for Honeycomb and increasing mean responses for the other two patterns.

Table 1. Maximum recorded torque by configuration.

Infill Pattern	Infill density (%)	A (N.m)	B (N.m)	C (N.m)	Mean ± SD (N.m)
Honeycomb	15	0.77	0.67	0.71	0.717 ± 0.050
Honeycomb	30	0.82	0.84	0.87	0.843 ± 0.025
Honeycomb	45	0.97	0.96	0.98	0.970 ± 0.010
Honeycomb	60	0.52	0.49	0.57	0.527 ± 0.040
Gyroid	15	0.77	0.73	0.61	0.703 ± 0.083
Gyroid	30	0.76	0.76	0.79	0.770 ± 0.017
Gyroid	45	0.81	0.83	0.78	0.807 ± 0.025
Gyroid	60	0.84	0.85	0.78	0.823 ± 0.038
Concentric	15	0.78	0.78	0.79	0.783 ± 0.006
Concentric	30	0.83	0.84	0.83	0.833 ± 0.006
Concentric	45	0.78	0.93	0.87	0.860 ± 0.075
Concentric	60	0.93	0.88	0.89	0.900 ± 0.026

Figure 2 shows the mean responses and the observed variation. SD ranged from approximately 0.006 N·m for Concentric at 15% and 30% to 0.083 N·m for Gyroid at 15%. Concentric at 45% also exhibited appreciable variation (SD = 0.075 N·m). Small SD values in some conditions describe agreement among the three tested specimens and should not be interpreted as proof of reproducibility across production batches.

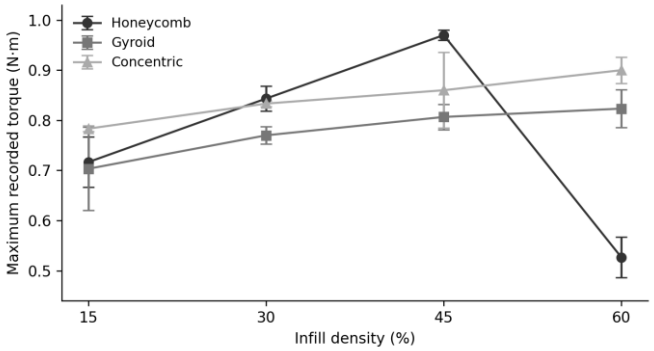


Figure 2. Mean maximum recorded torque versus infill density.

Across patterns, pooled mean maximum torque was 0.734, 0.816, 0.879 and 0.750 N·m at 15%, 30%, 45% and 60%, respectively. The mean at 60% was approximately 14.7% lower than at 45%. This pooled reduction is driven by Honeycomb and should not be generalised to Gyroid or Concentric, whose means increased at 60%. Additional internal material may alter load-bearing paths, but density alone does not describe their arrangement or deformation. The present experiment did not directly measure the structural mechanism responsible for the Honeycomb reduction.

NATIONAL ENGITECH DIGEST

VOL. 3 ISSUE 1

e-ISSN: 3030-5969

b. Effects of density and pattern

The factorial ANOVA results are presented in Table 2. Density was associated with maximum torque, $F(3,24) = 22.909$, $p < 0.001$, as was pattern, $F(2,24) = 13.013$, $p < 0.001$. The density–pattern interaction was significant, $F(6,24) = 24.249$, $p < 0.001$. The strong interaction is consistent with the different responses at 60%, especially the decrease in Honeycomb compared with the continued increases in Gyroid and Concentric. Therefore, a density recommendation or pattern ranking must refer to the specific combination tested.

Table 2. Two-factor ANOVA for maximum recorded torque using all 36 specimen values.

Source	df	Sum of squares	Mean square	F	p
Infill density	3	0.118364	0.039455	22.909	<0.001
Infill pattern	2	0.044822	0.022411	13.013	<0.001
Density × pattern	6	0.250578	0.041763	24.249	<0.001
Residual	24	0.041333	0.001722	—	—

The supplementary one-way density analysis yielded $F(3,32) = 3.749$, $p = 0.020$. Tukey comparisons detected a difference between 15% and 45% ($p = 0.026$). Other pooled density comparisons were not significant: 15%–30% ($p = 0.352$), 15%–60% ($p = 0.988$), 30%–45% ($p = 0.564$), 30%–60% ($p = 0.535$) and 45%–60% ($p = 0.055$). These comparisons average across patterns and therefore do not replace the interaction-based interpretation. A non-significant comparison does not establish equivalence.

Pooled pattern means were 0.764 N·m for Honeycomb, 0.776 N·m for Gyroid and 0.844 N·m for Concentric. A separate one-way pattern analysis did not reach significance, $F(2,33) = 1.803$, $p = 0.181$. This differs from the factorial pattern result because the one-way model absorbs density and interaction variation into its error term. The factorial model accounts for these sources explicitly and is the primary analysis for experimental design. Its significant interaction means that the pooled pattern means should not be used to identify a universal best pattern.

The data does not establish an optimal density for material efficiency. Specimen mass, print time and material consumption were not measured for this comparison. Although lower density is a potential resource-saving design choice, an efficiency claim would require these quantities alongside mechanical performance. The highest tested density should likewise not be treated as an optimum beyond the investigated 15%–60% range.

c. Torque at large recorded angular displacement

Table 3 compares torque at 1800° with mean peak torque for configurations with complete endpoint records. Concentric retained the greatest proportion at 15%, 45% and 60%, whereas Gyroid retained the greatest proportion at 30%. Concentric at 60% produced the highest complete-record mean endpoint torque, 0.840 ± 0.010 N·m, corresponding to 93.3% of its mean peak torque. Gyroid at 60% retained 0.100 N·m, or 12.1%. At 45%, Concentric retained 79.8%, compared with 11.0% for Honeycomb and 45.0% for Gyroid. The configuration with the highest mean peak torque, Honeycomb 45%, therefore differed from the configuration with the highest mean torque at the recorded endpoint, Concentric 60%.

Table 3. Torque at a recorded displacement of 1800° and retention relative to mean maximum torque. Endpoint n is the number of available readings; peak n = 3 for every configuration.

Pattern	Infill density (%)	Endpoint n	T_{1800} mean ± SD (N·m)	Retention (%)
Honeycomb	15	3	0.117 ± 0.029	16.3
Honeycomb	30	3	0.270 ± 0.210	32.0
Honeycomb	45	3	0.107 ± 0.012	11.0
Honeycomb	60	1	Not estimated	Not estimated
Gyroid	15	3	0.467 ± 0.015	66.4
Gyroid	30	3	0.547 ± 0.222	71.0
Gyroid	45	3	0.363 ± 0.235	45.0
Gyroid	60	3	0.100 ± 0.000	12.1
Concentric	15	3	0.590 ± 0.050	75.3
Concentric	30	3	0.130 ± 0.053	15.6
Concentric	45	3	0.687 ± 0.110	79.8
Concentric	60	3	0.840 ± 0.010	93.3

Honeycomb 60%: A and B have no reading at 1800°; the sole available C reading is −0.36 N·m. No three-specimen mean, SD or configuration retention ratio is estimated for this endpoint. Missing values are not imputed. Sustained torque after the peak indicates continued resistance during the recorded rotation. However, torque–angle measurements alone do not distinguish plastic deformation, interlayer damage and other contributions to the post-peak response. A detailed account of these mechanisms would require additional deformation measurements and fracture characterization. The endpoint comparison therefore complements peak torque without assigning a specific failure mechanism.

For a component whose principal requirement is peak resistance under comparable test conditions, Honeycomb at 45% is the leading configuration in this dataset. For resistance sustained to the recorded endpoint, Concentric at 60% warrants further investigation. The substantial reduction in Honeycomb peak torque at 60% cautions against assuming that higher nominal density always improves performance. Neither result directly establishes suitability for a complete functional product: geometry, service load, repeated loading and failure criteria require separate assessment.

d. Scope and limitation

The principal limitation is the small number of replicates. Three specimens permit preliminary comparisons and reporting of dispersion but provide uncertain estimates of population means and variances and cannot describe between-batch fabrication variability. A confirmatory study should define a practically relevant difference and estimate the required sample size using independent pilot variance information.

Conclusion

Thirty-six FDM-printed PLA specimens were tested across four infill densities and three patterns, with three replicates per configuration. The factorial analysis identified a significant density–pattern interaction, showing that the effect of density depends on architecture. Honeycomb at 45% achieved the highest mean maximum torque, 0.970 ± 0.010 N·m, but its mean decreased at 60%. Concentric at 60% achieved the highest mean torque at 1800° among configurations with complete endpoint records, retaining approximately 93% of its mean peak torque. The study demonstrates why peak torque and endpoint torque retention should be assessed separately and why increasing infill density cannot be assumed to improve torsional performance uniformly. Larger replicated tests are needed to establish general design recommendations.

References

Acierno, D., & Patti, A. (2023). Fused deposition modelling (FDM) of thermoplastic-based filaments: Process and rheological properties—An overview. Materials, 16(24), 7664.

Al-Tamimi, A. A., Pandžić, A., & Kadrić, E. (2023). Investigation and prediction of tensile, flexural, and compressive properties of tough PLA material using definitive screening design. Polymers, 15(20), 4169.

Cano-Vicent, A., Tambuwala, M. M., Hassan, S. S., Barh, D., Aljabali, A. A., Birkett, M., ... & Serrano-Aroca, Á. (2021). Fused deposition modelling: Current status, methodology, applications and future prospects. Additive manufacturing, 47, 102378.

Hatwalne, P. A., & Bhalerao, S. V. (2025). Numerical investigation of torsional analysis of 3D-printed PLA components using finite element analysis. In EPJ Web of Conferences (Vol. 341, p. 01052). EDP Sciences.

Joseph, T. M., Kallingal, A., Suresh, A. M., Mahapatra, D. K., Hasanin, M. S., Haponiuk, J., & Thomas, S. (2023). 3D printing of polylactic acid: recent advances and opportunities. The International Journal of Advanced Manufacturing Technology, 125(3), 1015-1035.

Kaya, H., & Yaman, U. (2026). Torsional characteristics of a novel infill pattern in material extrusion type of additive manufacturing: random lines. Progress in Additive Manufacturing, 11(1), 1261-1272.

Lumsden, G., Sarpong, J., & Khanafer, K. (2026). Cyclic Torsional Behavior of 3D-Printed ABS: Role of Infill Density and Raster Orientation. Machines, 14(3), 328.

Rajan, K., Samykano, M., Kadirgama, K., Harun, W. S. W., & Rahman, M. M. (2022). Fused deposition modeling: process, materials, parameters, properties, and applications. The International Journal of Advanced Manufacturing Technology, 120(3), 1531-1570.

Sadaghian, H., Khodadoost, S., Seifiasl, A., & Buswell, R. A. (2024). Preliminary insight into torsion of additively-manufactured polylactic acid (PLA)-based polymers. Experimental Mechanics, 64(9), 1443-1464.

Solomon, I. J., Sevvel, P., & Gunasekaran, J. J. M. T. P. (2021). A review on the various processing parameters in FDM. Materials Today: Proceedings, 37, 509-514.

Tanveer, M. Q., Mishra, G., Mishra, S., & Sharma, R. (2022). Effect of infill pattern and infill density on mechanical behaviour of FDM 3D printed Parts-a current review. Materials today: proceedings, 62, 100-108.